



CASCADED INVERTERS WITH SYNCHRONIZED MODULATION FOR TRANSFORMER-BASED PHOTOVOLTAIC INSTALLATION

Valentin OLESCHUK, Vladimir ERMURATSKII

Institute of Power Engineering of the Academy of Sciences of Moldova, Chisinau, Republic of Moldova

Abstract – This paper presents results of research of modulation processes in power conversion system with triple voltage source inverters, supplied by photovoltaic (PV) strings, and connected to a transformer. Four-winding transformer has in this case specific connections between the secondary windings and inverters, allowing providing of multilevel voltages at secondary windings of the transformer. Specialized space-vector-based strategy of pulsewidth modulation (PWM) has been used for control of inverters, insuring quarter-wave symmetry of winding voltages for any modulation indices and switching frequency of inverters. Analysis and comparison of harmonic composition of winding voltages and output voltages of inverters has been done on the base of simulation of system with three basic variants of the scheme of synchronized modulation.

Keywords – voltage source inverter, photovoltaic panels and strings, modulation scheme, voltage synchronization

INVERTOARE DE TIP CASCAD CU MODULAȚIE SINCRONĂ PENTRU INSTALAȚIE FOTOVOLTAICĂ CU TRASFORMATOR

Valentin OLESCIUK, Vladimir ERMURATSCHI

Institutul de Energetica al Academiei de Stiinta a Moldovei, Chisinau, Republica Moldova

Rezumat – Lucrarea prezintă rezultatele cercetării proceselor de modulare în sistemul de conversie a energiei în baza invertoarelor triple, care se alimentează de la circuite fotovoltaice, și racordate cu un transformator de putere cu patru înfășurări. Transformatorul se caracterizează printr-o schemă de conectare specifică între înfășurările secundare și invertoare, care permite formarea tensiunii de ieșire pe mai multe niveluri pe înfășurările secundare ale transformatorului. Schema modulării vectoriale sincrone utilizată pentru dirijarea și reglarea invertoarelor, asigură simetria sfertului de undă a tensiunii pe înfășurările secundare pentru orice indici de modulație și frecvență de comutare a invertoarelor. Analiza comparativă a compoziției armonice a tensiunii de ieșire a invertoarelor și tensiunii pe înfășurările secundare ale transformatorului s-a realizat în baza simulării sistemului cu trei variante ale modulației sincrone.

Cuvinte cheie – inverter de tensiune, panouri și circuite fotovoltaice, schema de modulare, sincronizare formelor tensiunii.

КАСКАДНО-СВЯЗАННЫЕ ИНВЕРТОРЫ С СИНХРОННОЙ МОДУЛЯЦИЕЙ ДЛЯ ФОТОПРЕОБРАЗОВАТЕЛЬНОЙ УСТАНОВКИ ТРАНСФОРМАТОРНОГО ТИПА

В. Олещук, В. Ермуратский

Институт энергетики Академии наук Молдовы, Кишинев, Республика Молдова

Реферат – Представлены результаты анализа модуляционных процессов в преобразовательной системе на базе строенных инверторов, питающихся от трех фотопреобразовательных цепей, и связанных с силовым трансформатором. Четырехобмоточный трансформатор характеризуется при этом специальной схемой соединения вторичных обмоток с инверторами, благодаря чему на вторичных обмотках формируется многоуровневое выходное напряжение. Схема синхронной векторной модуляции, использованная для управления и регулирования инверторов, обеспечивает при этом четвертьволновую симметрию напряжений на вторичных обмотках трансформатора при любых значениях коэффициентов модуляции и частот коммутации инверторов. Выполнено моделирование процессов в системе с тремя разновидностями синхронной векторной модуляции, проведен сопоставительный анализ гармонического состава базовых форм напряжения на выходе инверторов и на вторичных обмотках трансформатора.

Ключевые слова – инвертор напряжения, фотопреобразовательные панели и цепи, стратегия и тактика модуляции.

1. INTRODUCTION

Development of photovoltaic-focused power conversion systems is growing rapidly. Novel transformer-less and transformer-based topologies and configurations of solar

photovoltaic installations for solar farms and solar factories have been proposed and investigated [1]-[4].

Recently, modified structure of transformer-based system with triple three-phase voltage source inverters has been proposed [5],[6]. Fig. 1 shows topology of this system for the case of delta-connection of secondary windings,

supplied by three insulated strings of photovoltaic panels. Fig. 2 presents the corresponding secondary windings for the case of star-connection [6]. It has been shown in [6], that simple modification of connection between outputs of standard two-level inverters and windings of the transformer allow providing multilevel winding voltages for systems with insulated dc-sources. Also, winding voltages can be expressed in this case by the phase voltages of triple inverters. Operation of inverter-based photovoltaic systems is in dependence of the used methods and techniques of PWM.

Space-vector modulation is perspective method for control of inverters, including PV application. During system operation, for some regimes of photovoltaic systems (grid frequency fluctuation, different voltages of strings of PV panels, etc.) it is necessary to ensure voltage synchronization. So, this paper presents results of research of modulation processes in PV system with triple transformer-connected inverters, controlled by specialized schemes and techniques of space-vector PWM, insuring voltage synchronization and voltage symmetries for any operating conditions of the system.

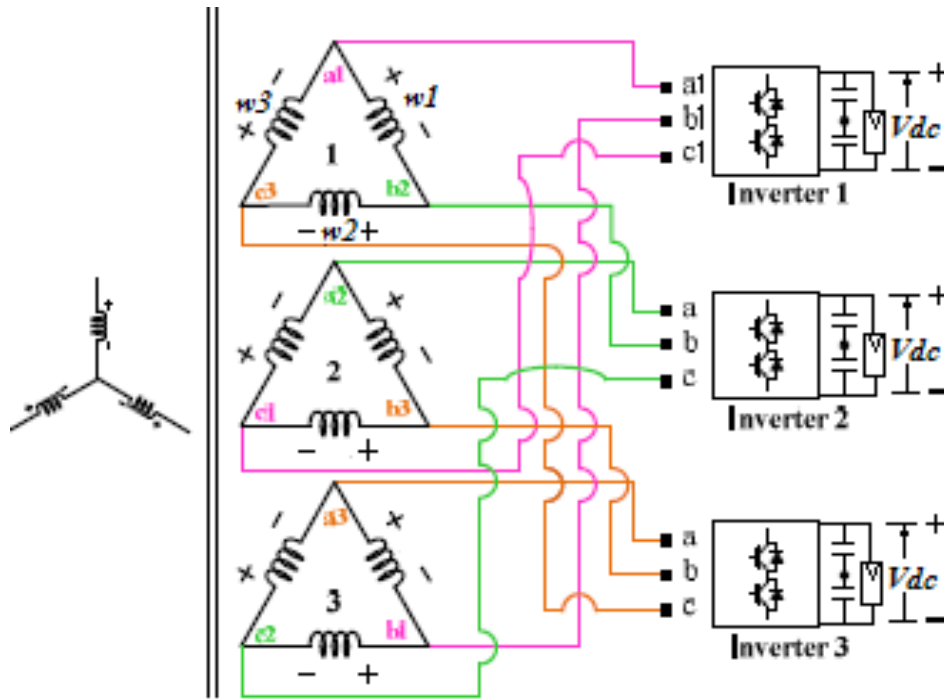


Fig. 1. Topology of transformer-based photovoltaic system with triple inverters specifically connected to secondary windings of the transformer (case of delta connection of windings).

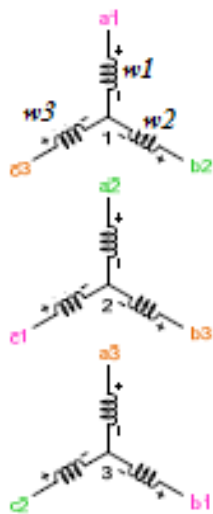


Fig. 2. Secondary windings of transformer of the system for the case of star-connection.

2. TWO-LEVEL INVERTERS WITH SYNCHRONOUS SPACE-VECTOR MODULATION

To assure voltage synchronization and waveform symmetries of inverters, specialized method of space-vector modulation can be used for control of triple inverters of PV system. Table I presents peculiarities and the main control dependences of this method of synchronous modulation, which are compared here with the corresponding parameters of conventional space-vector PWM [7]-[9].

Table 1 - Basic Parameters of PWM Methods

Control (modulation) parameter	Conventional schemes of space-vector PWM	Specialized method of modulation	
Operating and max parameter	Operating & max voltage V and V_m	Operating & maximum fundamental frequency F and F_m	
Modulation index m	V / V_m	F / F_m	
Duration of sub-cycles	T	τ	
Center of the k -signal	α_k (angles/degr.)	$\tau(k-1)$ (sec)	
Switch-on durations	$T_{ak} = 1.1mT[\sin(60^\circ - \alpha_k) + \sin \alpha_k]$ $t_{ak} = 1.1mT \sin \alpha_k$ $t_{bk} = 1.1mT \times \sin(60^\circ - \alpha_k)$	Algebraic PWM	Trigonomet-ric PWM
		$\beta_k = \beta_1[1 - A \times (k-1)\tau FK_{ov1}]$ $\gamma_k = \beta_{i-k+1}[0.5 - 6(i-k)\tau F]K_{ov2}$ $\beta_k - \gamma_k$	$\beta_k = \beta_1 \times \cos[(k-1)\tau K_{ov1}]$ $\gamma_k = \beta_{i-k+1}[0.5 - 0.9m(i-k)\tau]K_{ov2}$ $\beta_k - \gamma_k$
Switch-off states (zero voltage)	$t_{0k} = T - t_{ak} - t_{bk}$	$\lambda_k = \tau - \beta_k$	
Special parameters providing synchronization of the process of PWM		$\beta'' = \beta_1[1 - A \times (k-1)\tau FK_{ov1}]K_s$ $\lambda' = (\tau - \beta'') \times K_{ov1}K_s$	$\beta'' = \beta_1 \times \cos [(k-1)\tau K_{ov1}]K_s$ $\lambda' = (\tau - \beta'') \times K_{ov1}K_s$

3. SYNCHRONOUS PWM OF INVERTERS IN TRIPLE-INVERTER-BASED SYSTEM

Phase voltages V_{as1} , V_{bs1} and V_{cs1} of the first standard three-phase inverter (**Inverter 1** in Fig. 1) of the system are calculated in accordance with (1)-(3) [7]:

$$V_{as1} = V_{a10} + (V_{a10} + V_{b10} + V_{c10})/3 \quad (1)$$

$$V_{bs1} = V_{b10} + (V_{a10} + V_{b10} + V_{c10})/3 \quad (2)$$

$$V_{cs1} = V_{c10} + (V_{a10} + V_{b10} + V_{c10})/3, \quad (3)$$

where V_{a10} , V_{b10} and V_{c10} are the corresponding pole voltages of the first inverter.

Winding voltages of secondary windings of the system (V_{w1} , V_{w2} , V_{w3} in Fig. 1) can be expressed by the phase voltages of triple inverters in accordance with (4)-(9) [6]. Dependences (4)-(6) correspond to the case of delta-connection of windings, presented in Fig. 1, dependences (7)-(9) correspond to the case of star-connection, presented in Fig. 2.

$$V_{w1} = V_{as3} - V_{bs1} \quad (4)$$

$$V_{w2} = V_{bs1} - V_{cs2} \quad (5)$$

$$V_{w3} = V_{cs2} - V_{as3} \quad (6)$$

$$V_{w1} = 0.667V_{as1} - 0.333V_{bs2} - 0.333V_{cs3} \quad (7)$$

$$V_{w2} = -0.333V_{as1} + 0.667V_{bs2} - 0.333V_{cs3} \quad (8)$$

$$V_{w3} = -0.333V_{as1} - 0.333V_{bs2} + 0.667V_{cs3} \quad (9)$$

Control and output signals of triple inverters of the system are shifted by 120° (120° interleaving in accordance with some definitions). Also, small additional shift between control signals of three inverters, equal to $1/3$ of duration of the switching period (switching sub-cycle) has been provided by the used scheme of control and modulation.

Fig. 3 – Fig. 13 .present results of simulation of processes in the system on the base of triple synchronously modulated inverters, and show basic voltage waveforms (pole voltages V_{a10} , V_{b10} , V_{c10} of the first inverter, phase V_{as1} and line-to-line V_{a1b1} voltages of the first inverter, and also winding voltages $V_{w1phase}$ and V_{w1line} , corresponding to the cases of star-connection and delta-connection of windings). It present also spectra of the phase V_{as1} and line V_{a1b1} voltages of inverters, and also spectra of winding voltages $V_{w1phase}$ and V_{w1line} .

Figs. 3-4 show voltage waveforms and voltage spectra of the system controlled in accordance with scheme of continuous synchronous modulation [7]. The fundamental frequency of the system is equal to $F=50Hz$, and switching frequency is equal to $F_s=1.13kHz$. Modulation index is equal to $m=0.65$ in this case.

Figs. 5-7 present voltage waveforms and the corresponding voltage spectra of system controlled by the scheme of synchronous discontinuous space-vector PWM with the 30° -non-switching intervals ([7], DPWM30, $F=50Hz$, average $F_s=1.13kHz$, $m=0.75$).

Figs. 8-9 illustrate modulation processes in system controlled by scheme of synchronous discontinuous

space-vector PWM with the 60° -non-switching intervals ([7], DPWM60, $F=50\text{Hz}$, average $F_s=1.13\text{kHz}$, $m=0.85$). Figs. 10-13 illustrate regimes of operation of inverters with discontinuous PWM in two parts of the zone of overmodulation (Figs. 10-11: the first part of the zone of modulation – DPWM60, $F=50\text{Hz}$, average $F_s=1.13\text{kHz}$, $m=0.95$; Figs. 12-13: the second part of the overmodulation zone – DPWM30, $F=50\text{Hz}$, average $F_s=1.13\text{kHz}$, $m=0.975$).

To emphasize properties of the used specialized scheme of PWM, fractional frequency ratio between the switching and fundamental frequencies (equal to $1130\text{Hz}/50\text{Hz}= 22.6$) has been used. Analysis of harmonic composition of symmetrical (with quarter-wave symmetry) voltage waveforms of the system shows (see Figs. 6-13), that spectra of the all presented waveforms do not include even harmonics and subharmonics for any values of modulation indices of inverters.

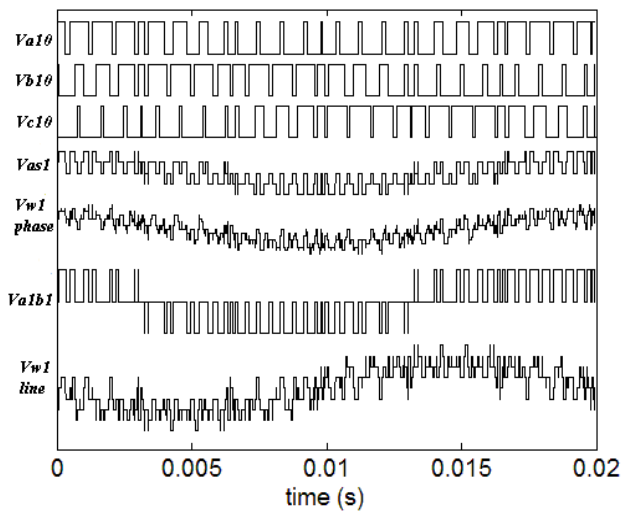


Fig. 3. Pole voltages $V_{a1\theta}$, $V_{b1\theta}$, $V_{c1\theta}$, phase voltage V_{as1} , line voltage V_{alb1} of the first inverter, and the corresponding winding voltages $V_{w1phase}$ and V_{w1line} of the system with continuous synchronous PWM (CPWM, $F=50\text{Hz}$, $F_s=1.13\text{kHz}$, $F_s/F=24.6$, $m=0.65$).

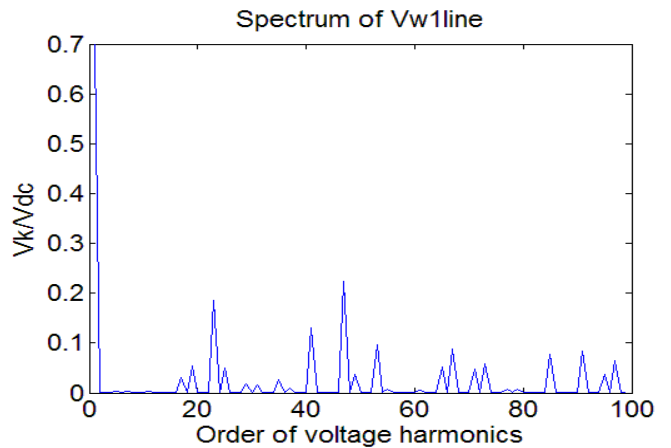
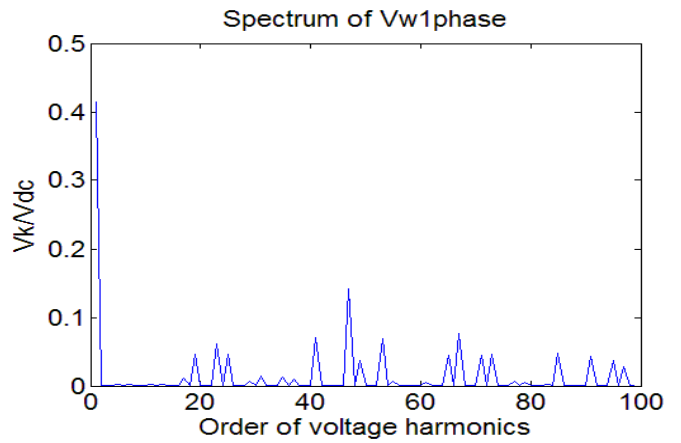
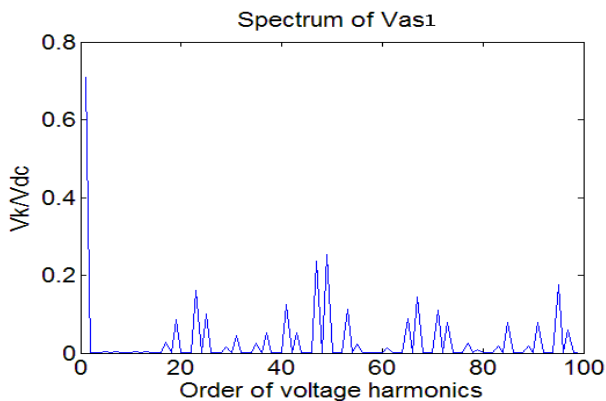


Fig. 4. Spectra of voltage waveforms of the system with continuous synchronous PWM ($F=50\text{Hz}$, $F_s=1.13\text{kHz}$, $m=0.65$).

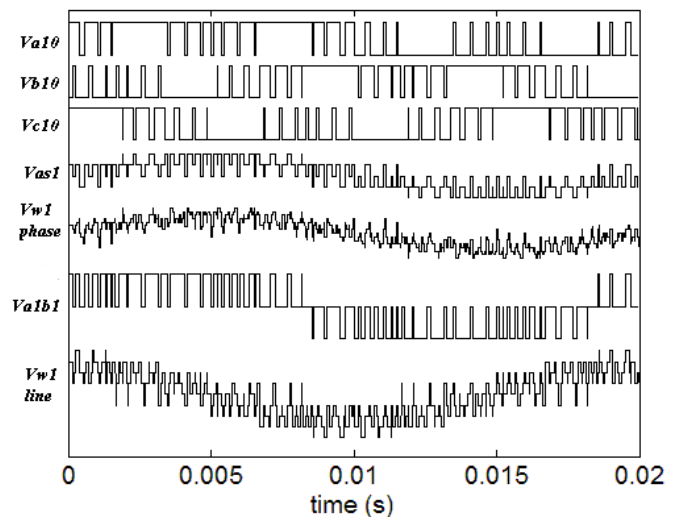


Fig. 5. Pole voltages $V_{a1\theta}$, $V_{b1\theta}$, $V_{c1\theta}$, phase voltage V_{as1} , line voltage V_{alb1} of the first inverter, and the corresponding winding voltages $V_{w1phase}$ and V_{w1line} of the system with discontinuous synchronous PWM (DPWM30, $F=50\text{Hz}$, $F_s=1.13\text{kHz}$, $F_s/F=24.6$, $m=0.75$).

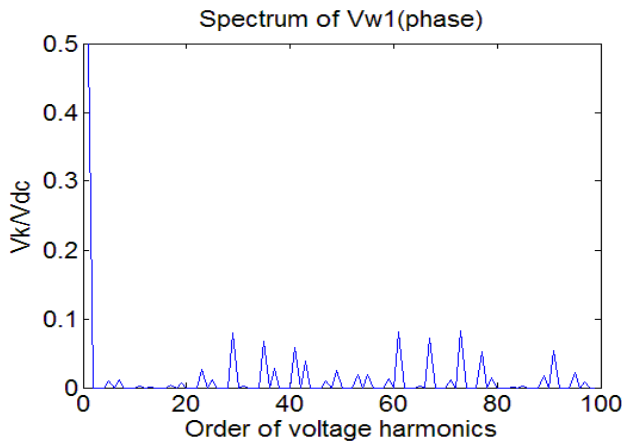
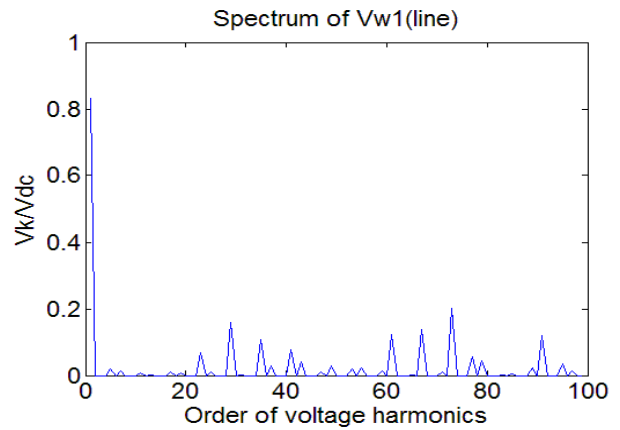
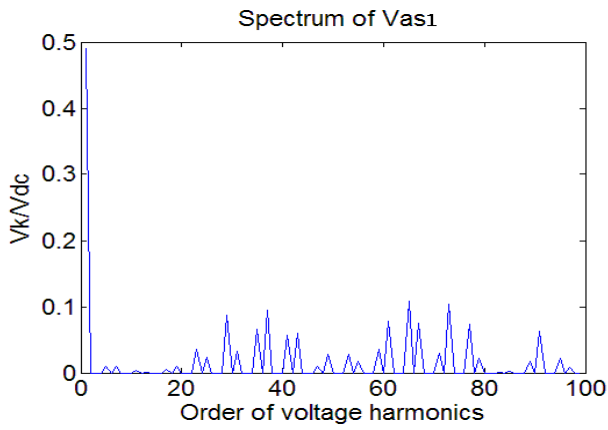


Fig. 6. Spectra of voltage waveforms of the system with discontinuous PWM (DPWM30, $F=50\text{Hz}$, $F_s=1.13\text{kHz}$, $m=0.75$).

Total Harmonic Distortion factor is an important criterion for analysis and comparison of voltage waveforms in photovoltaic systems. In particular, for 50-Hz systems it has been recommended to take into consideration harmonics up to the 40th voltage harmonic for determination of total voltage harmonic distortion factor [10]. Figs. 14-15-present results of calculation of Total Harmonic Distortion factor (THD) for basic voltage waveforms of the system as function of modulation index m of triple inverters, controlled by synchronous techni-

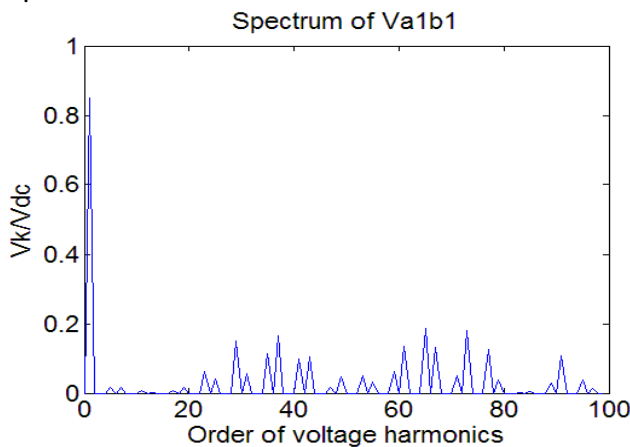


Fig. 7. Spectra of voltage waveforms of the system with discontinuous PWM (DPWM30, $F=50\text{Hz}$, $F_s=1.13\text{kHz}$, $m=0.75$).

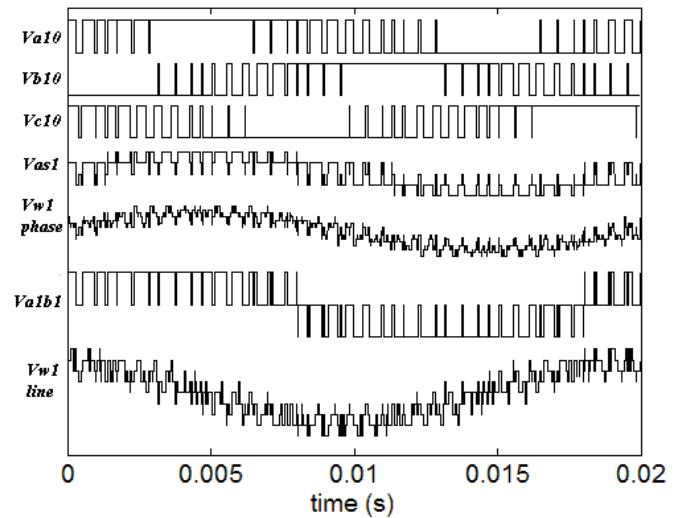
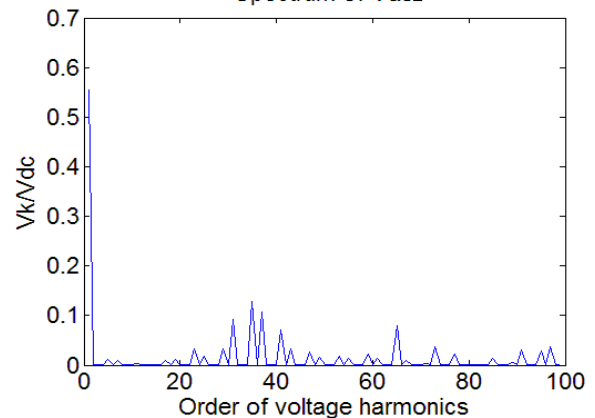


Fig. 8. Pole voltages $V_{a1\theta}$, $V_{b1\theta}$, $V_{c1\theta}$, phase voltage V_{as1} , line voltage V_{a1b1} of the first inverter, and the corresponding winding voltages $V_{w1\text{phase}}$ and $V_{w1\text{line}}$ of the system with discontinuous synchronous PWM (DPWM60, $F=50\text{Hz}$, $F_s=1.13\text{kHz}$, $F_s/F=24.6$, $m=0.85$).

ques of continuous (CPWM) and discontinuous (DPWM30 and DPWM60) modulation. THD factor has been calculated until the 40-th low-order (k -th) voltage

harmonic (Fig. 14, $THD = (1/V_{w1_1}) \sqrt{\sum_{k=2}^{40} V_{w1_k}^2}$), and also

until the 1000-th harmonic of voltage spectra (Fig. 15, Spectrum of V_{as1}



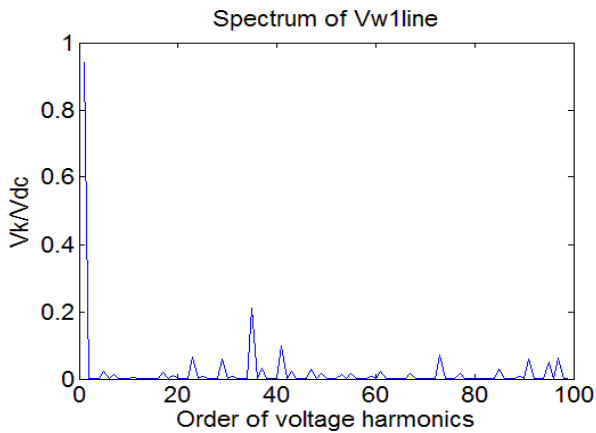
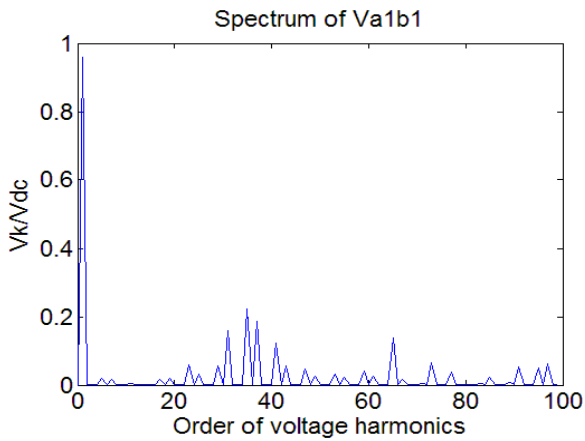
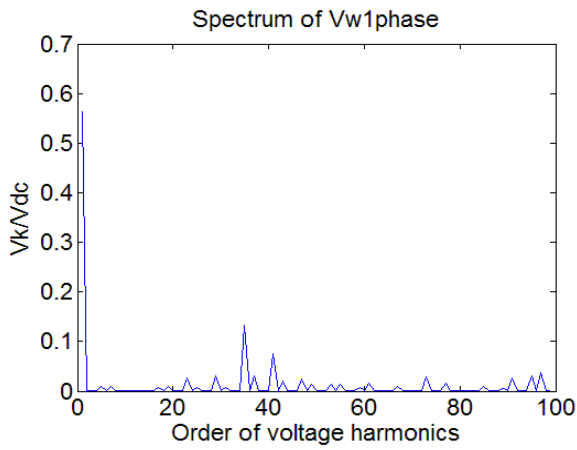


Fig. 9. Spectra of voltage waveforms of the system with discontinuous PWM (DPWM60, $F=50\text{Hz}$, $F_s=1.13\text{kHz}$, $m=0.85$).

$$THD = (1/V_{w1_1}) \cdot \sqrt{\sum_{k=2}^{1000} V_{w1_k}^2}$$

The fundamental frequency of the system was equal to 50Hz , and the average switching frequency of triple inverters was equal to 1.4kHz .

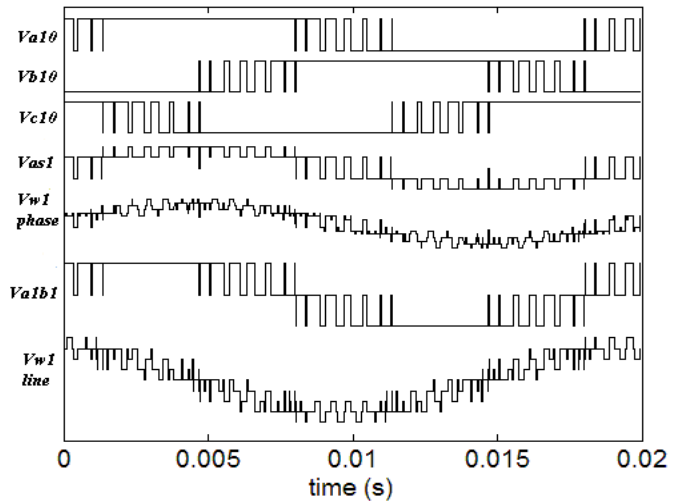


Fig. 10. Pole voltages $V_{a1\theta}$, $V_{b1\theta}$, $V_{c1\theta}$, phase voltage V_{as1} , line voltage V_{a1b1} of the first inverter, and the corresponding winding voltages $V_{w1\text{phase}}$ and $V_{w1\text{line}}$ of the system with discontinuous synchronous PWM in the overmodulation zone (DPWM60, $F=50\text{Hz}$, $F_s=1.13\text{kHz}$, $F_s/F=24.6$, $m=0.95$).

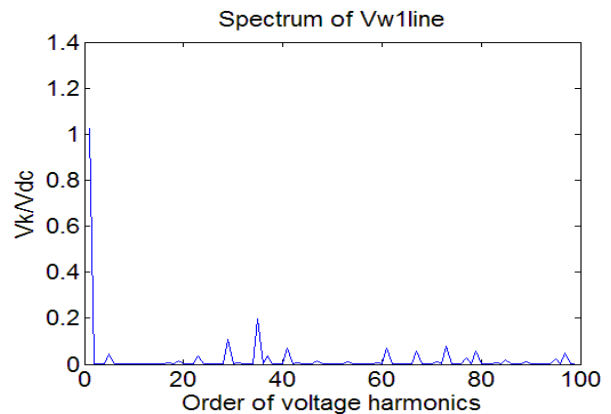
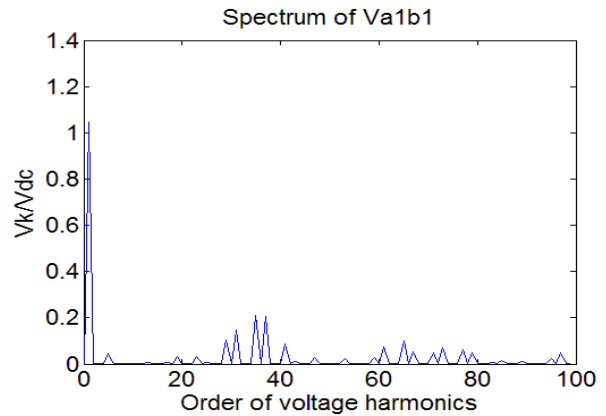


Fig. 11. Spectra of voltage waveforms of the system with discontinuous PWM (DPWM30, $F=50\text{Hz}$, $F_s=1.13\text{kHz}$, $m=0.95$).

Analysis of the presented in Fig. 14 and Fig. 15 results of calculation of THD factor shows, that due to the proposed in [6] connection between triple inverters and the secondary windings of the transformer, there is appreciable improvement of integral spectral characteristics of winding voltages. As an example, in accordance with diagram of Fig. 14 (for the case, if

$m=0.7$), THD factor for winding voltages is reduced by 14% (for system with algorithm of CPWM), by 8% (for system controlled by algorithm of DPWM30), and by

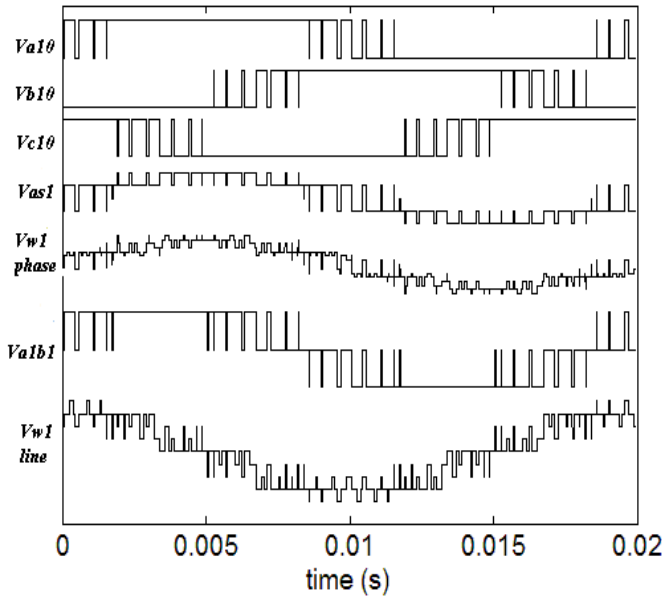


Fig. 12. Pole voltages V_{a10} , V_{b10} , V_{c10} , phase voltage V_{as1} , line voltage V_{a1b1} of the first inverter, and the corresponding winding voltages $V_{w1phase}$ and V_{w1line} of the system with discontinuous synchronous PWM in the overmodulation zone (DPWM30, $F=50\text{Hz}$, $F_s=1.13\text{kHz}$, $F_s/F=24.6$, $m=0.975$).

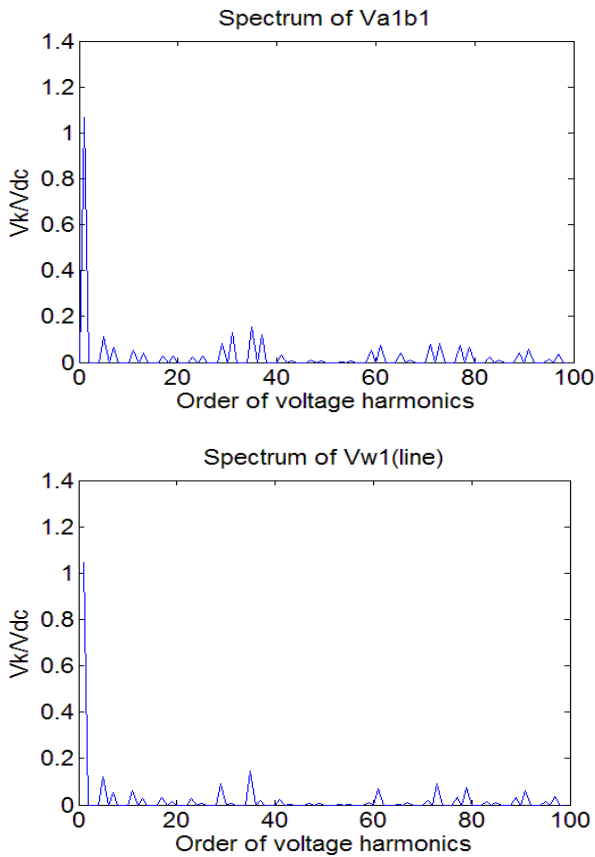


Fig. 13. Spectra of voltage waveforms of the system with discontinuous synchronous PWM (DPWM30, $F=50\text{Hz}$, $F_s=1.13\text{kHz}$, $m=0.975$).

63% for system with DPWM60, in comparison with the corresponding line voltages. Accordingly, data of the diagram, presented in Fig. 15, show (as an example, for the case, if $m=0.7$), that THD factor for winding voltages of system with new connection between inverters and transformer is decreased by 23% (for system with

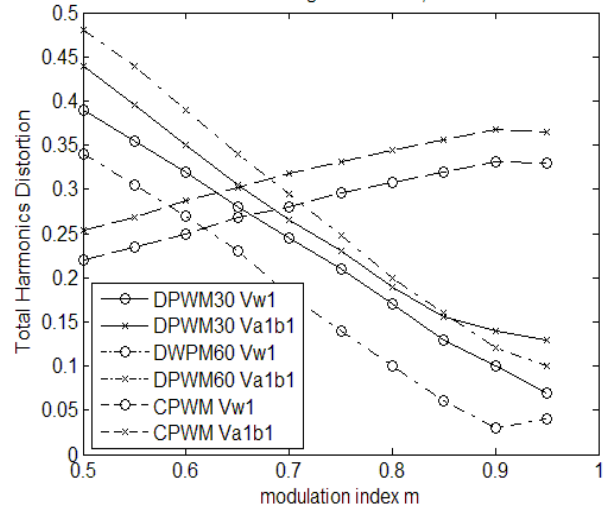


Fig. 14. THD factor of voltages of the system versus modulation index m ($k=40$).

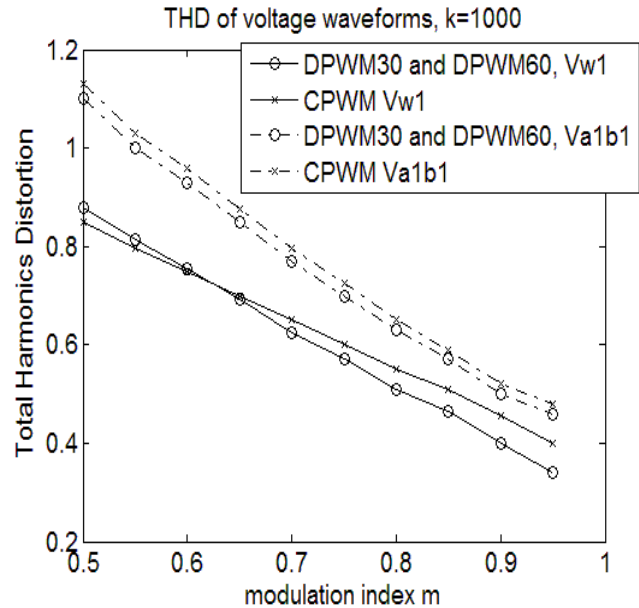


Fig. 15. THD factor of voltages of the system versus modulation index m ($k=1000$).

DPWM30 or DPWM60), and by 22% (for system controlled by algorithm of CPWM), in comparison with the corresponding line voltages (case of conventional connection between inverters and transformer).

So, improved spectral composition of winding voltages of transformer-based system assures to reduce copper loss in windings of the transformer, and also to decrease switching and conduction losses at triple inverters.

4. CONCLUSION

Specialized schemes and techniques of feedforward space-vector modulation, insuring voltage synchronization and voltage symmetries of inverters, can be used effectively in transformer-based photovoltaic systems on the base of triple inverters with novel connection between inverters and windings of the transformer.

The presented voltage spectrograms illustrate qualitatively and quantitatively attenuation of the corresponding harmonics of winding voltages due to new connections inside the system.

To emphasize properties of the used specialized scheme of pulsewidth modulation, fractional frequency ratio between the switching frequency and fundamental frequency (equal to $1130\text{Hz}/50\text{Hz}=22.6$) has been chosen for analysis of modulation processes in system. Research of harmonic composition of symmetrical (with quarter-wave symmetry) voltage waveforms of the system shows (see Figs. 6, 7, 9, 11, 13), that spectra of the all presented waveforms do not include even harmonics and subharmonics for any values of modulation indices of inverters operating at both linear control zone and zone of overmodulation.

It has been shown, that in general case *THD* factor for winding voltages of secondary windings of the system with new connection between inverters and transformer is decreased (in average) by about 20% for systems with both continuous and discontinuous synchronous pulsewidth modulation, in comparison with the case of conventional connection between inverters and transformer.

REFERENCES

- [1] G. Grandi, C. Rossi, D. Ostojic, and D. Casadei, "A new multilevel conversion structure for grid-connected PV applications," *IEEE Trans. Ind. Electron.*, vol. 56, no. 11, 2009, pp. 4416–4426.
- [2] G. Spagnuolo, et al., "Renewable Energy Operation and Conversion Schemes", *IEEE Industrial Electronics Magazine*, vol. 4, no. 1, 2010, pp. 38-51.
- [3] V. Oleschuk and G. Griva, "Simulation of processes in synchronized cascaded inverters for photovoltaic application," *International Review of Electrical Engineering*, vol. 4, no. 5, 2009, pp. 975-982.
- [4] *Renewable Energy. Selected Issues*, vol. 2. Cambridge Scholars Publishing, 2016, pp. 166-247.
- [5] Yongsoon Park, Sungjae Ohn, and Seung-Ki Sul, "Multi-level operation with two-level converters through a double-delta source connected transformer," *Journal of Power Electronics*, vol. 14, no. 6, 2014, pp. 1093-1099.
- [6] Sungjae Ohn, Yongsoon Park, and Seung-Ki Sul, "Multi-level operation of triple two-level PWM converters," *Proc. of IEEE Energy Conversion Congress and Exposition (ECCE'2015)*, 2015, pp. 4283-4289.
- [7] F. Blaabjerg, V. Oleschuk, and F. Lugeanu, "Synchronization of output voltage waveforms in three-phase inverters for induction motor drives," *Proc. of IEEE-IEEJ Power Conversion Conf. (PCC'2002)*, 2002, pp. 528-533.
- [8] V. Oleschuk, G. Grandi, and P. Sanjeevikumar, "Simulation of processes in dual three-phase system on the base of four inverters with synchronized modulation," *Advances in Power Electronics*, vol. 2011, 2011, pp. 1-9.
- [9] V. Oleschuk and F. Barrero, "Standard and non-standard approaches for voltage synchronization of drive inverters with space-vector PWM: A survey," *International Review of Electrical Engineering*, vol. 9, no. 4, 2014, pp. 688-707.
- [10] M. Aiello, A. Cataliotti, S. Favuzza, and G. Graditi, "Theoretical and experimental comparison of Total Harmonic Distortion factors for the evaluation of harmonic and interharmonic pollution of grid-connected photovoltaic systems," *IEEE Trans. Power Delivery*, vol. 21, no. 3, 2006, pp. 1390-1397.